Contents lists available at ScienceDirect

# Biochimica et Biophysica Acta

journal homepage: www.elsevier.com/locate/bbagen

Review

# Structural insight into the PTS sugar transporter EIIC☆

Jason G. McCoy, Elena J. Levin, Ming Zhou *

Verna and Marrs McLean Department of Biochemistry and Molecular Biology, Baylor College of Medicine, Houston, TX 77030, USA

## ARTICLE INFO

## ABSTRACT

*Background:* The enzyme IIC (EIIC) component of the phosphotransferase system (PTS) is responsible for selectively transporting sugar molecules across the inner bacterial membrane. This is accomplished in parallel with phosphorylation of the sugar, which prevents efflux of the sugar back across the membrane. This process is a key part of an extensive signaling network that allows bacteria to efficiently utilize preferred carbohydrate sources.
*Scope of review:* The goal of this review is to examine the current understanding of the structural features of the EIIC and how it mediates concentrative, selective sugar transport. The crystal structure of an N,N′-diacetylchitobiose transporter is used as a structural template for the glucose superfamily of PTS transporters.
*Major conclusions:* Comparison of protein sequences in context with the known EIIC structure suggests that members of the glucose superfamily of PTS transporters may exhibit variations in topology. Despite these differences, a conserved histidine and glutamate appear to have roles shared across the superfamily in sugar binding and phosphorylation. In the proposed transport model, a rigid body motion between two structural domains and movement of an intracellular loop provide the substrate binding site with alternating access, and reveal a surface required for interaction with the phosphotransfer protein responsible for catalysis.
*General significance:* The structural and functional data discussed here give a preliminary understanding of how transport in EIIC is achieved. However, given the great sequence diversity between varying glucose-superfamily PTS transporters and lack of data on conformational changes needed for transport, additional structures of other members and conformations are still required. This article is part of a Special Issue entitled: Structural biochemistry and biophysics of membrane proteins.

## 1. Introduction

The PTS is a multiple component carbohydrate uptake system that drives specific saccharides across the bacterial inner membrane while simultaneously catalyzing sugar phosphorylation. The proteins composing the PTS include a series of soluble phosphotransferases, and an integral membrane protein responsible for transport of the sugar into the cell. The phosphorylation state of the soluble components is indicative of intracellular carbohydrate levels and provides a mechanism for regulating carbohydrate metabolism [1–3]. In this review we discuss the structural basis for the functions of the transmembrane component of the PTS, including recognition of the cognate substrate, the mechanism of transport, and its role in catalyzing the phosphotransfer reaction. We focus on the glucose superfamily of PTS transporters, including the recently solved structure of the N,N′-diacetylchitobiose transporter, bcChbC, as well as the *Escherichia coli* transporters PtsG (glucose

transporter), MtlA (mannitol transporter), and BglF (β-glucoside transporter) as the best-characterized representatives of their respective families.

### 1.1. Classification of PTS transporters

Phylogenetic analysis indicates that PTS transporters originate from at least four independent sources [4,5]. Of these four superfamilies, the glucose superfamily of PTS transporters is the largest and the primary focus of this review [4,6]. Five distinct subfamilies of proteins have been identified within the glucose superfamily: the lactose family, the glucose family, the β-glucoside family, the mannitol family, and the fructose family [6]. It has been suggested that the fructose-specific transporter is the oldest, followed by the mannitol-specific transporter [5]. The glucose and β-glucoside transporters show greater similarity to each other than to the fructose and mannitol transporters and the lactose transporters are the most divergent [5]. Though homologous, the PTS transporters of different family members show a great deal of sequence diversity. For example, the transport domains of bcChbC, PtsG, MtlA, and BglF only share between 17 and 19% identity between them. Although the families are named for specific sugars, the selectivity

of individual members within each family can vary considerably. For instance, the bcChbC protein is a member of the lactose family, but is selective for N,N′-diacetylchitobiose.

### 1.2. Components and organization of the phosphotransferase system

The PTS is composed of several proteins that serially transfer a phosphate moiety until it is ultimately attached to a sugar molecule (Fig. 1A). The glycolytic intermediate phosphoenolpyruvate provides the initial phosphate [7] which is then transferred to enzyme I (EI), heat-stable phosphocarrier protein (HPr), and subsequently to enzyme II (EII). EII is composed of three separate domains named EIIA, EIIB, and EIIC. The phosphate is serially transferred from HPr to EIIA, and then to EIIB. The number of phosphate inversions as measured through isotopic substitution indicates that the phosphate is then transferred directly from EIIB to the sugar without formation of a covalent EIIC-phosphate intermediate; however, this transfer only occurs when the sugar is bound to EIIC [8]. Bacteria typically contain multiple PTS systems for uptake of different sugars. EI and HPr are not selective and are shared by different PTS systems. In contrast to EI and HPr, EIIA and EIIB have been shown to have different folds between different subfamilies of the PTS glucose superfamily and are not interchangeable [9–16].

The EIIA, EIIB, and EIIC domains can be expressed as a single protein or as distinct polypeptides (Fig. 1B). The order of connected domains varies as well. While bcChbC consists of just the EIIC domain, the β-glucoside transporter BglF is composed of an N-terminal EIIB followed by EIIC and then EIIA [17], the mannitol transporter MtlA contains EIIC followed by EIIB and EIIA [18], and the glucose transporter PtsG contains an EIIC domain followed by an EIIB [19]. This variability occurs even within individual subfamilies. For example, the *E. coli* glucose family member TreB (trehalose transporter) has the EIIB domain before the EIIC. The connectivity and arrangement of these domains appears to have effects on function. For the glucose transporter PtsG,

separation of the EIIB and EIIC components leads to a 50-fold decrease in phosphotransfer [20], and scrambling the order of domains in BglF from BCA to CBA prevents phosphotransfer to the sugar [21].

## 2. The structure of EIIC

The membrane-embedded EIIC domain forms a dimer [22–24] and is responsible for selective binding and transport of sugar molecules [18,25,26]. While many NMR and crystallographic structures of EIIA and EIIB domains have been reported, including the isolated domains [9–16], complexes with each other [27–29], and complexes with other transporters [30]; obtaining high resolution structures of the EIIC domain has proven difficult. Previous efforts have resulted in EM projection maps of MtlA (5 Å) and PtsG (12 Å), both of which confirmed the dimeric assembly of the EIIC but were of insufficient resolution to provide atomic level information about the protein [31,32]. The first 3D crystal structure of an EIIC domain was reported in 2011 [24]. The structure of bcChbC, an N,N′-diacetylchitobiose transporter from *Bacillus cereus* (PDB ID: 3QNQ), was solved to a resolution of 3.3 Å and is described below [24].

### 2.1. Overall fold of bcChbC

The bcChbC protein contains just the EIIC component, and its corresponding EIIB and EIIA are encoded by separate genes [33]. The protein was purified in detergent and eluted from a gel filtration column as a dimer. Each monomer consisted of 10 transmembrane (TM) helices with the N and C termini facing the cytoplasmic side of the protein. These transmembrane domains form two separate domains: the N-terminal oligomerization domain made up of TM1–5, and a C-terminal transport domain containing TM6–10 (Figs. 2 and 3). These two domains are connected by an amphipathic helix (AH2) on the periplasmic side of the membrane. The C-terminal domain also contains two reentrant helical hairpins. The first reentrant loop is located on the cytoplasmic side between TM8 and 9 and contains two helices, HP1a and HP1b. The second reentrant loop is between TM9 and 10 on the periplasmic side, and contains only one helix (HP2). TM8 is split into two helices connected by a short, flexible loop (TM8a and TM8b).

The bcChbC dimerization interface has an expansive buried surface area of 2746 Å$^2$ (Fig. 2A). The dimer has approximate 2-fold symmetry along an axis perpendicular to the plane of the membrane. Most of the interface is mediated by TM helices 1, 2, 3, and 5 from the N-terminal domain of each monomer. Unlike the extensive interface between the two protomers, the interface between the N-terminal oligomerization and C-terminal transport domains is quite small due to the presence of a large cavity in both monomers lined by TM 1, 6, 7, and 8, HP1b, the loop preceding HP2, and the TM4–TM5 loop from the other monomer. This cavity contains a bound N,N′-diacetylchitobiose molecule in each protomer. Consequently the oligomerization and sugar transport/phosphorylation functionality appear to be segregated to the N- and C-terminal domains respectively. One exception to this is the TM4–TM5 loop, which extends across the N-terminal domain of its dimeric partner to make contact with both N,N′-diacetylchitobiose and HP1b within the other protomer (Fig. 2A).

### 2.2. The ligand binding site in bcChbC

The N,N′-diacetylchitobiose binding site is formed by helices TM6, TM7, HP1b, TM8, and the reentrant loop containing HP2 in both bcChbC monomers (Fig. 2B). The nonreducing monomer of the N,N′-diacetylchitobiose disaccharide has extensive interactions with the protein. OH-6 forms hydrogen bonds with E334 on HP1b and H250 on the cytoplasmic loop connecting TM6 and TM7, while OH-3 and OH-4 form hydrogen bonds with the sidechain and backbone amide of N333 from HP1b. N-2 forms a hydrogen bond with the backbone carbonyl of G297 on TM8. OH-7 forms a hydrogen
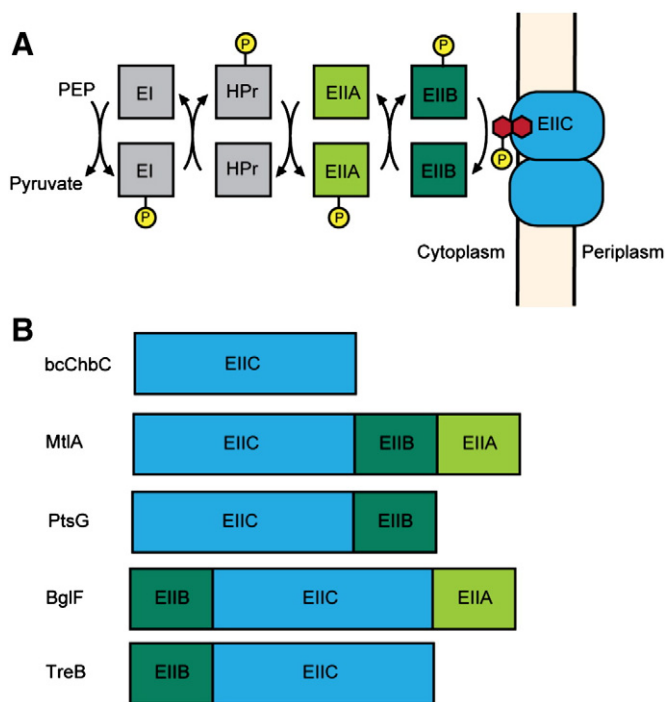


**Fig. 1.** Organization of the PTS. A. Flow diagram illustrating sequence of phosphorylation events leading to the addition of phosphate (yellow) to the EIIC transporter-bound sugar molecule (red). B. The EIIC domain can be translated individually or as a multidomain protein containing EIIB and/or EIIA.
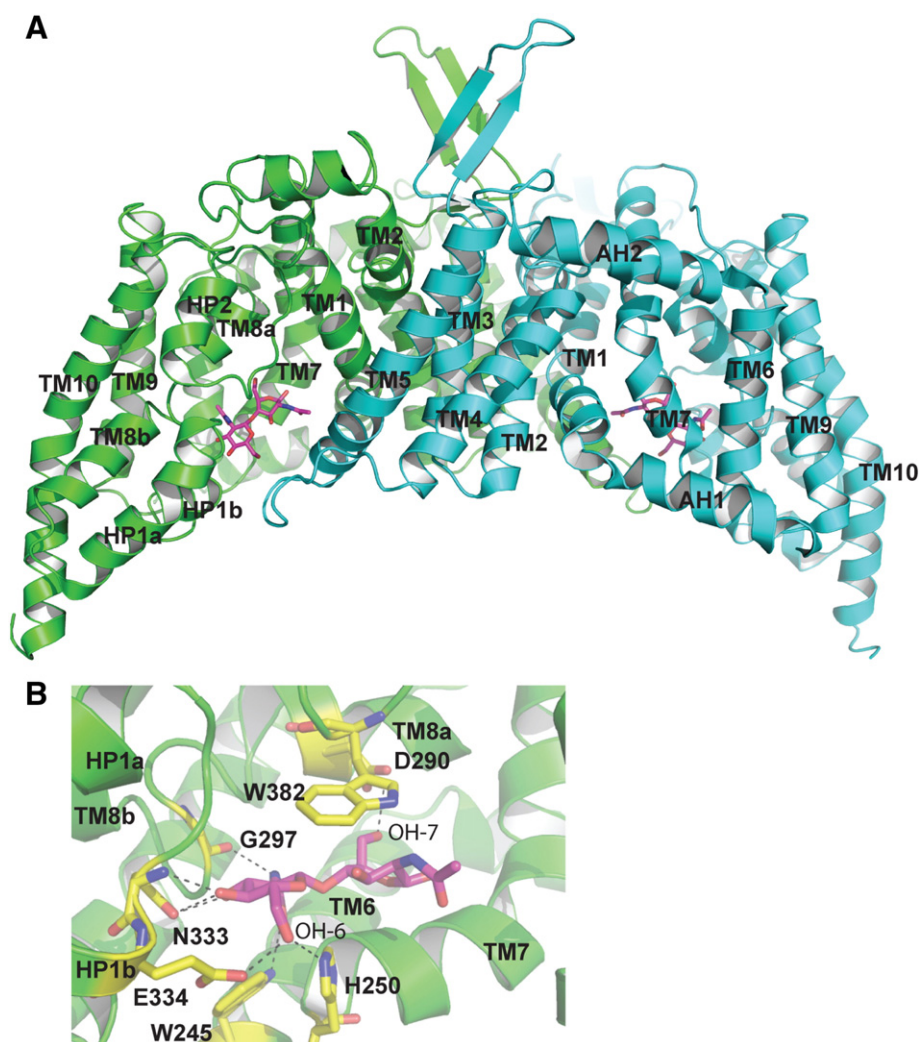
**Fig. 2.** The bcChbC structure. A. The two protomers of the bcChbC dimer are colored green and cyan. Each monomer contains a molecule of N,N′-diacetylchitobiose. Each protomer contains two domains: an N-terminal dimerization domain made up of TM1 through TM5 and a C-terminal domain in which transport and phosphorylation occur containing TM6–10. B. The N,N′-diacetylchitobiose binding site. Interacting residues are colored yellow and originate from TM6, TM7, HP1b, TM8, and the reentrant loop containing HP2.

bond with W245 from the end of TM6. W382 from the second reentrant loop packs tightly against the face of the disaccharide to form stabilizing stacking interactions. On the reducing end of the disaccharide, the only interaction with the protein is a hydrogen bond between D290 from TM8a and OH-7. The cavity itself is considerably larger than N,N′-diacetylchitobiose and could potentially accommodate an N-acetylglucosamine trisaccharide, which can be transported by *E. coli* ChbC [34]. No openings on either the periplasmic or cytoplasmic side are of sufficient size to allow egress of the disaccharide from the protein.

Residues H250 and E334 are strongly conserved in other PTS glucose superfamily members. Mutation of these residues can dramatically impact both binding and phosphorylation of the sugar. In MtlA, mutation of H195 to an arginine or alanine reduced PEP-dependent phosphorylation roughly 20-fold, whereas an H195N mutation showed wild-type activity [35]. All three mutations greatly reduced affinity for the ligand [36]. In PtsG the H212Q mutation lowered the phosphotransferase activity to only 15% of the wild type protein [37]. In BglF, H306 was also shown to be essential for phosphate transfer to the sugar [17]. E257A and E257Q mutants of the mannitol transporter showed no binding to mannitol while an E257D mutation resulted in binding and phosphate transfer with only 3% of the wild type maximal rate [38,39]. The position of these residues in bcChbC provides clues as to the topology of other

EIIC proteins and suggests a possible mechanism for sugar phosphorylation. Both of these issues are addressed below.

## 3. Conservation of the PTS glucose superfamily fold across different subfamilies

### 3.1. Previous topology models of the glucose superfamily

Given the low identity between different subfamilies in the glucose superfamily, the question arises whether all glucose superfamily EIIC members contain 10 transmembrane helices and two reentrant loops as in bcChbC, or whether there are topology differences between (and perhaps within) different family members. Prior to the solution of the bcChbC structure, Saier et al. suggested that all glucose superfamily members might share a common topological fold based on an extensive bioinformatics analysis covering over 200 homologs within the glucose superfamily [6]. Their model, which is based on charge distribution and hydropathy plots, is very similar to the experimental structure of bcChbC. They predicted the presence of 8 transmembrane helices with two reentrant loops, a cytoplasmic reentrant loop following TM6 and a periplasmic reentrant loop following TM7, with both the N- and C-termini on the cytoplasmic side of the protein. Their model differs
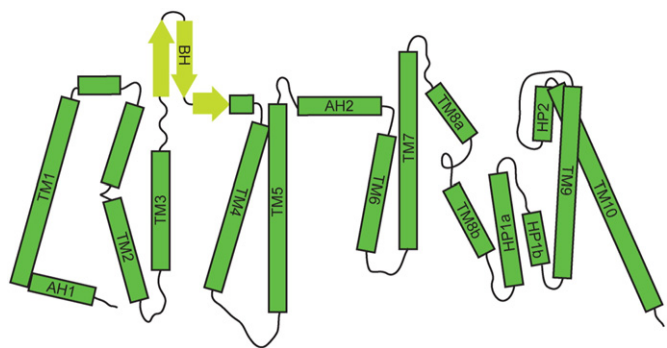
**Fig. 3.** Topology diagram of the bcChbC monomer. The bcChbC protomer contains ten transmembrane helices and two reentrant loops. The protein is oriented with the periplasmic side on top, and helices are indicated with green rectangles. Beta sheets are indicated with yellow arrows. The N-terminal oligomerization domain and the C-terminal transport domain are separated by a periplasmic amphipathic helix (AH2).

from bcChbC only by the absence of TM4 and TM7 from the bcChbC structure.

In the PtsG transporter, a member of the glucose family, Buhr and Erni found evidence of 8 transmembrane helices using a combination of hydropathy analysis and PhoA and LacZ gene fusions [40]. They predicted a large cytoplasmic loop between TM6 and TM7. A similar overall topology with an even larger cytoplasmic loop was proposed for the

BglF transporter, a member of the β-glucoside family, based on hydrophobic analysis and extensive cysteine mutagenesis and labeling [41, 42]. They further predicted two cytoplasmic reentrant loops in the large cytoplasmic loop between TM6 and TM7. In contrast, for the MtlA transporter, a member of the mannitol family, initial hydropathy analysis predicted the presence of 7 transmembrane helices in the EIIC with a large cytoplasmic loop between helices 6 and 7 [43]. Alternatively, phoA gene fusions to MtlA suggested the presence of 6 transmembrane helices with large cytoplasmic loops between TM2 and 3 and TM4 and 5 [44]. Further cysteine mutagenesis and sulfhydryl labeling studies indicated that these large loops probably reenter the membrane in the form of reentrant loops [45]. The 6 transmembrane domain topology has been further supported by steady-state tryptophan fluorescence studies [46] and a 5 Å electron crystallography projection structure that revealed 6 regions of high density [32].

### 3.2. The bcChbC structure suggests different topologies for glucose superfamily members

We conclude that different topological arrangements exist based on the structure of bcChbC [24], hydropathy analysis with TMHMM [47], and manual alignment of the sequences for bcChbC, PtsG, BglF, and MtlA. The manual alignment in Fig. 4 is based on predictions by TMHMM (displayed with red text), the topology models described above (sequence outlined in black box), and a sequence motif identified by Nguyen et al. (sequence outlined in pink box) [6]. This motif contains
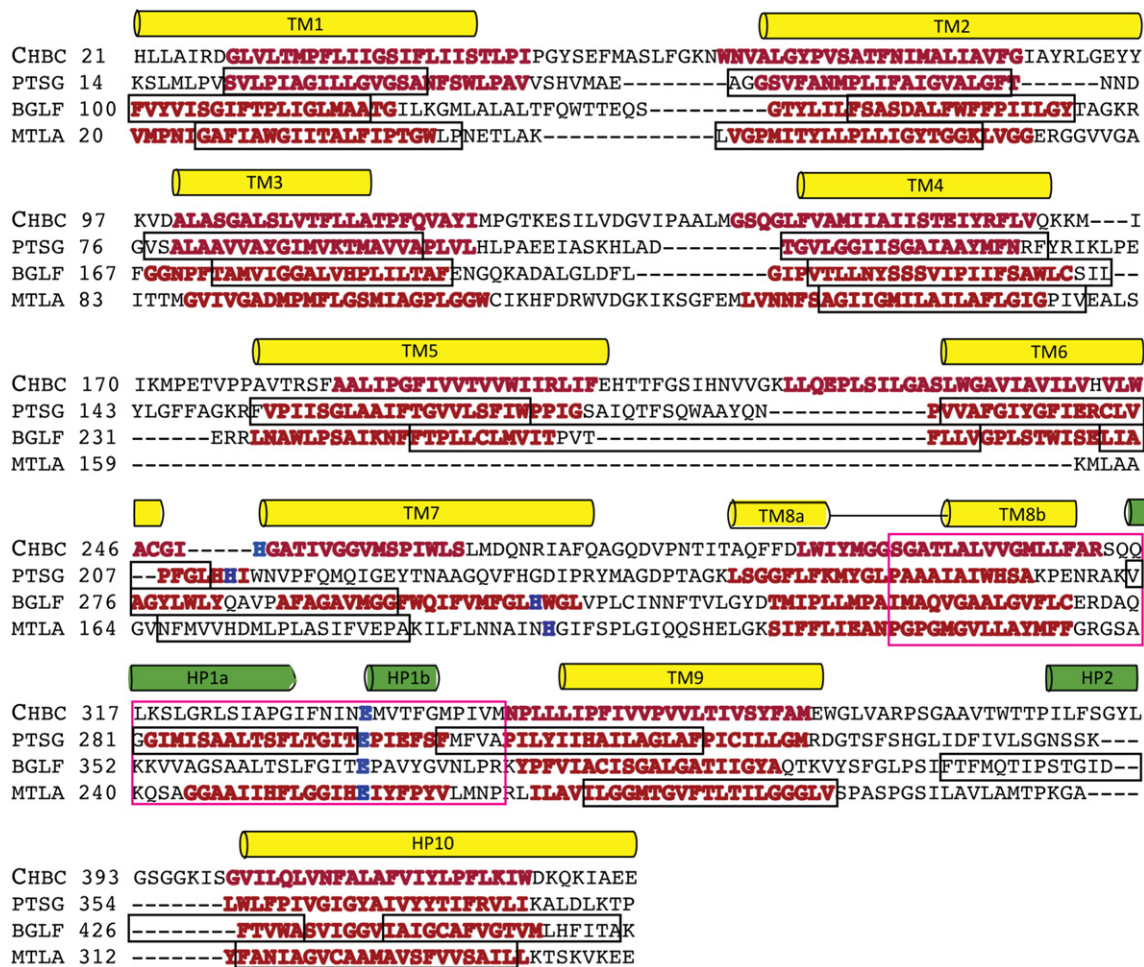


**Fig. 4.** Alignment of the EIIC domain of four glucose superfamily members based on transmembrane helix prediction by TMHMM. Predicted transmembrane helices are in red. Transmembrane helices observed in the bcChbC crystal structure are in yellow, reentrant loop helices are in green, and E334 and H250 in bcChbC are in blue. Predicted helices from gene fusion and cysteine labeling experiments are in black boxes. The conserved region identified by Nguyen et al. is highlighted with a pink box.

the highly conserved glutamate (E334 in bcChbC, shown in blue in Fig. 4). In the bcChbC structure this motif corresponds to TM8b and the cytoplasmic reentrant loop that follows it. A second highly conserved residue (H250 in bcChbC) is also shown in blue in Fig. 4. This residue is located on the cytoplasmic loop preceding TM7. In the bcChbC structure the side chains of H250 and E334 form hydrogen bonds with the OH-6 group on the nonreducing monomer of the N,N′-diacetylchitobiose disaccharide, which receives the phosphate. Assuming that these two residues are involved in a phosphorylation mechanism conserved across the glucose superfamily, they must remain spatially close to the sugar hydroxyl group. As phosphate transfer occurs on the cytoplasmic side of the protein where the EIIB domain binds, these residues presumably need to be close to the cytoplasmic side of the membrane, as in bcChbC.

There are 83 residues separating E334 and H250 in bcChbC and 85 separating the homologous residues in PtsG. In bcChbC this span of residues crosses the membrane twice and forms a reentrant loop, placing both E334 and H250 on the cytoplasmic side. In contrast, there are only 62 and 61 residues separating the conserved glutamate and histidine in BglF and MtlA, respectively. Given the predicted locations of hydrophobic regions shown in Fig. 4 it is difficult to see how these two proteins can contain the same structural elements as bcChbC and maintain the spatial proximity of the conserved glutamate and histidine. Alternatively, both the topology model for BglF predicted by Yagur-Kroll and Amster-Choder [41] and the topology model for MtlA predicted by Sugiyama et al. [44] position the conserved glutamate and histidine on the cytoplasmic surface of the protein by not including any transmembrane passes between them. Additional evidence of topological differences comes from crosslinking studies in both BglF and MtlA, which indicated close proximity of residues that are separated in the bcChbC structure [42,48]. For example, in MtlA, out of 6 different single residue cysteine mutations (MtlA residue numbers 47, 73, 124, 134, 187, and 270) that demonstrate crosslinking (indicating their presence near the oligomerization interface) only 2 of these (73 and 134) are anywhere near the dimer interface in bcChbC.

In contrast to MtlA and BglF, the sequence position of the conserved histidine relative to the conserved glutamate in PtsG is similar to that of bcChbC. Furthermore, the secondary structure of bcChbC fits well with the topology prediction by Buhr and Erni [40] and Nguyen et al. [6] for the first six transmembrane helices, placing the conserved histidine on the cytoplasmic surface of the protein. However, the variations in these models after TM6 would place the conserved glutamate at the periplasmic surface. Given the role in catalysis we expect these two residues play, we predict that this organization is unlikely. The TMHMM predicted transmembrane helices for PtsG align well with the bcChbC secondary structure for helices TM8, HP1, TM9 and TM10 (Fig. 4). Only bcChbC TM7 is not predicted for PtsG. Consequently, we expect that the topology of PtsG may be very similar to that of bcChbC, whereas the topology of both BglF and MtlA appears to be different.

### 3.3. Similarities between sugar binding in bcChbC and PtsG

The similarity in topology between bcChbC and PtsG extends to the sugar binding site as well. The N,N′-diacetylchitobiose binding site in bcChbC closely matches the molecular determinants described for glucose binding in PtsG. In a study by Garcia-Alles et al., various analogs of glucose were used to determine which functional groups on the sugar were required for binding [49]. The conserved bcChbC residues H250, E334, and N333, (N333 is most commonly a threonine in the glucose family) form hydrogen bonds with OH-6 and OH-4 that were shown to be critical for binding in PtsG. OH-3, which was shown to function as a hydrogen bond acceptor in PtsG, forms a hydrogen bond with the sidechain of N333 in bcChbC (equivalent to T297 in PtsG). OH-1 was shown to have no impact on binding in PtsG. In bcChbC the equivalent oxygen faces out into the cavity away from the surface of the protein. Alterations of the OH-2 group were also shown to reduce glucose binding

affinity in PtsG, but on N,N′-diacetylchitobiose the C2 position has an acetylamine group instead of a hydroxyl.

## 4. Mechanism of sugar phosphorylation

### 4.1. Phosphate transfer involves a complex with EIIB

Phosphorylation of the sugar requires the formation of a complex between EIIC and phosphorylated EIIB [50,51]. Crosslinking studies have been used to identify residues lining the EIIB–EIIC interface in MtlA [52] and ITC results suggest the interaction may involve up to 50 to 60 residues [51]; however, there is currently no available structure. NMR and crystal structures for both the phosphorylated and unphosphorylated *E. coli* ChbC-specific EIIB have been reported [9,53,54] as well as an NMR structure of the complex between the EIIB and EIIA components [27]. EIIB domains from other subfamilies in the glucose superfamily are structurally distinct and do not complement each other [9–16].

The ChbC-specific EIIB contains a 4-stranded parallel β-sheet made up of a repeating β–α–β motif with helices on both sides of the sheet [9]. The cysteine responsible for transferring the covalently bound phosphate resides on a loop following the initial β-strand. This loop has a similar structure to the phosphate-bearing loop in the low-molecular-weight phosphotyrosine protein phosphatase (LMWPTP), another enzyme that makes use of a covalent cysteinyl phosphate interaction [55]. In the EIIB–EIIA complex this loop is inserted into a gap between two helices within the EIIA. The EIIB makes contacts with both of these helices primarily through the loops and helical regions following the C-terminal ends of the β-strands, resulting in a buried surface area of 945 Å$^2$ [27].

In the absence of structural data for the bcChbC–bcChbB complex, we have attempted to manually dock an EIIB domain onto the bcChbC cytoplasmic surface. A homology model of bcChbB was generated with I-TASSER [56] using the phosphorylated ChbB structure from *E. coli* (PDB ID: 1H9C) [54]. Analysis of the surface of the bcChbB homology model reveals a positively charged pocket containing the covalently attached phosphate group (Fig. 5B). From the bcChbC structure the only obvious access point for the phosphate is directly through the gap between three helices: TM7 which contains H250, HP1b which contains E334, and TM5 from the opposing dimeric subunit. The electrostatic surface of bcChbC reveals a negatively charged sugar-containing cavity that directly complements the positive electrostatics of bcChbB (Fig. 5A). While correct placement of the phosphate cannot be achieved in the protein conformation observed in the crystal structure of bcChbC, repositioning of the TM4–TM5 loop from the other subunit provides enough space to bring the bcChbB model into a position from which the phosphate and sugar are sufficiently close for catalysis to occur (Fig. 5C). In this position it appears that HP1b, TM7, TM1, the loop between TM2 and TM3, and AH1 preceding TM1 may form contacts with the bcChbB subunit. This initial amphipathic helix aligns with one of the interacting helices from EIIA in the EIIA–EIIB complex structure. N-terminal amphipathic helices are nearly ubiquitous in EIICs and have been shown to be critical for proper incorporation into the membrane [57].

### 4.2. A putative mechanism for phosphorylation

In the bcChbC structure both H250 and E334 lie on the cytoplasmic side of the sugar and form hydrogen bonds with the OH-6 group of N,N′-diacetylchitobiose that is phosphorylated [34]. Given the similarity of the EIIB cysteine-containing loop to that of LMWPTP, the two enzymes may share mechanistic similarities. In the second half of the LMWPTP catalyzed reaction, a conserved aspartate acts as a general base, extracting a proton from a water molecule that then initiates a nucleophilic attack on the phosphorous covalently bound to cysteine [58]. The phosphate intermediate is stabilized by a conserved arginine through hydrogen bonded ionic interactions as well as positive dipoles contributed by surrounding helices [59]. In the bcChbC structure the conserved glutamate (E334) appears to be in a position to serve the
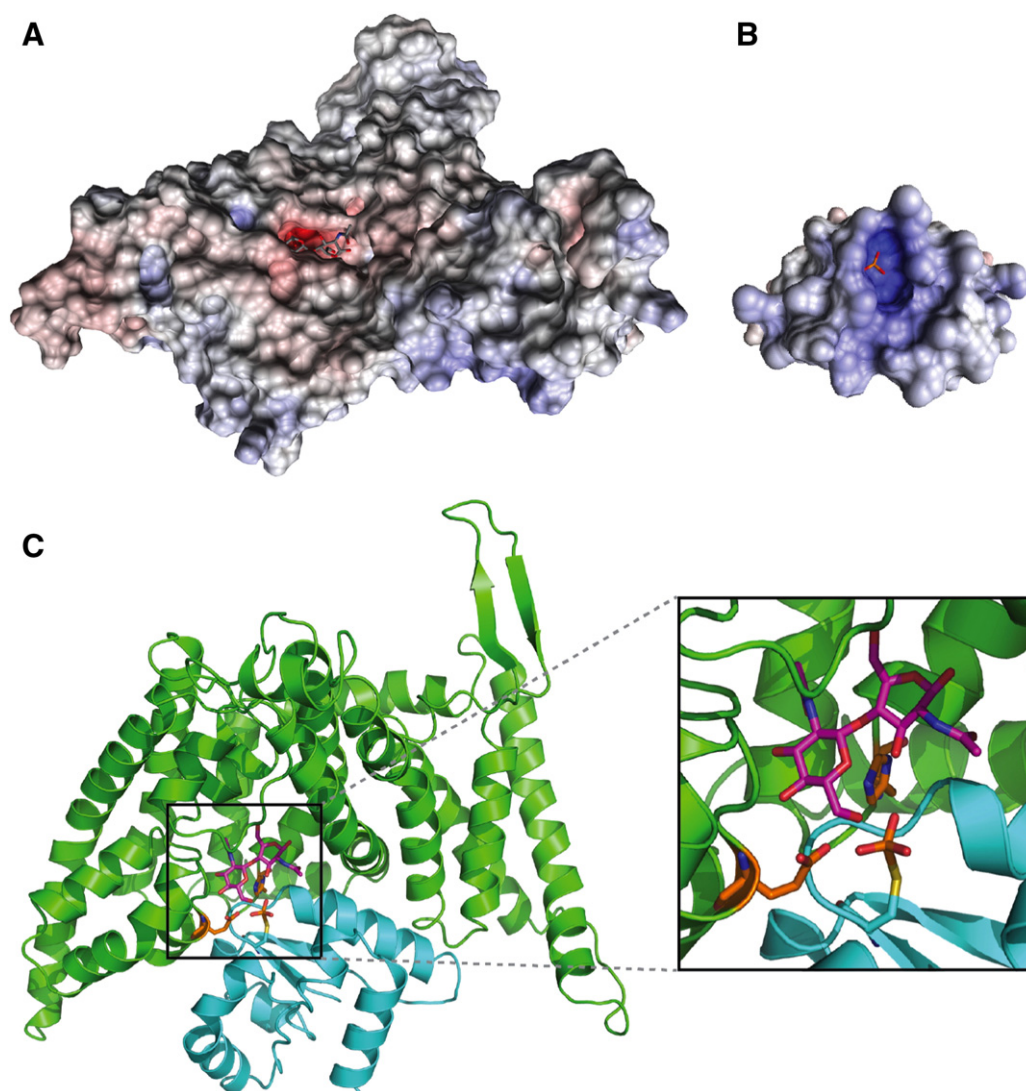
**Fig. 5.** Predicted model of the bcChbC–bcChbB complex. The electrostatic surfaces of A. bcChbC and B. a homology model of bcChbB are complementary. C. The predicted bcChbC (green) bcChbB (cyan) complex generated by manual docking. The cysteine attached phosphate is positioned directly below the O6 oxygen of maltose (magenta).

same function as the aspartate, extracting a proton from the C6 hydroxyl and priming it to attack the phosphate on the EIIB. The histidine may polarize the glutamate in order to activate it for base catalysis. A similar mechanism has been described for ATP hydrolysis in DNA gyrase [60]. The protonated histidine and positive helix dipoles contributed by TM7 and HP1b could then help to stabilize the phosphate intermediate. Following phosphorylation of the sugar, the increased negative charge of the phosphate would reduce the affinity of the negatively charged sugar binding site for the sugar, driving the release of the sugar into the cytoplasm.

## 5. Transport

To facilitate transport of their cognate ligands across the bilayer without permitting the non-specific leak of other solutes, transporters must alternate between at least two different conformations: an outward-open state, in which the substrate binding site is open to the extracellular space but inaccessible from the cytoplasm; and an inward-open state, in which the substrate binding site is blocked from the extracellular side but accessible to the cytoplasm. Intermediate states in which the ligand binding site is occluded from the solvent on both sides have also been observed. In addition, the EIIC transport

cycle involves complexation with the EIIB domain and phosphorylation of the transported sugar prior to its release into the cytoplasm.

### 5.1. Structure based model of transport

In the bcChbC structure the sugar is blocked from release into the periplasm and cytoplasm. The structure therefore corresponds to an occluded conformation. On the cytoplasmic side, N,N′-diacetylchitobiose is blocked by both the reentrant loop containing HP1a and HP1b as well as the loop between TM4 and TM5 of the other protomer. On the periplasmic side access is blocked by the second reentrant loop containing HP2 and TM8a. The structure of bcChbC suggests a possible mechanism of transport. The loosely connected oligomerization (TM1–TM5) and transport (TM6–TM10) domains appear well suited for interdomain rigid body motions, specifically an upwards translation and rotation of the transport domain that would shift HP2 and TM8a away from the oligomerization domain, opening the cavity to the periplasm while simultaneously closing off the cavity to the cytoplasm and shifting the sugar binding site closer to the periplasm (Fig. 6). A similar rigid body motion has been proposed for the glutamate transporter based on crystal structures of the inward open and outward open conformations [61].
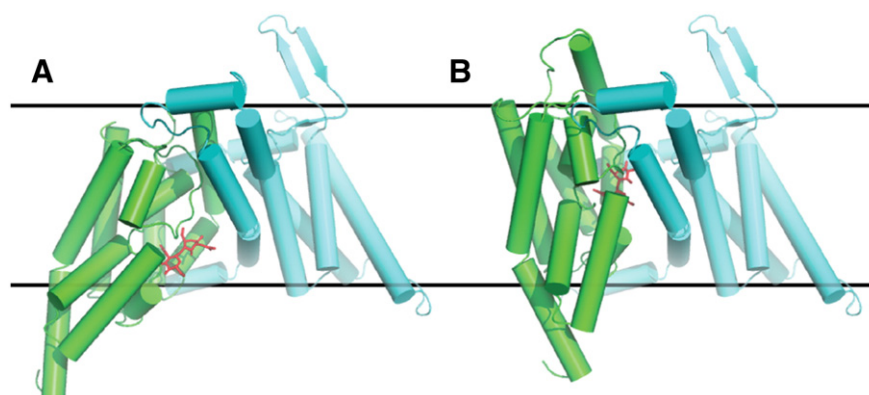
**Fig. 6.** Model of the (A) inward open ChbC monomer crystal structure and (B) predicted ChbC monomer outward open state involving a rigid body rotation and upwards translation of the transport domain (TM6–10, green) relative to the oligomerization domain (TM1–5, cyan).

Binding of saccharide to this outward open conformation would then drive a conformational change into the occluded conformation observed in the bcChbC crystal structure. Phosphorylated EIIB could then bind to the cytoplasmic surface of EIIC after movement of the TM4–TM5 loop away from the active site, catalyzing phosphorylation of the sugar. The EIIB–EIIC complex would then disengage, followed by release of the phosphorylated sugar.

### 5.2. Mutations that modify transport in PtsG

As we predict that bcCbhC and PtsG share a common topology, it may be possible to infer details about the translocation mechanism by mapping mutations made on PtsG that modify transport onto the structure of bcChbC. These mutations do in fact support the transport mechanism described above. Buhr et al. found multiple mutations in PtsG that significantly decreased transport activity, but had little effect on phosphorylation of the sugar [62]. These include M17T or I, G149S, K150E, S157F, H339Y, and D343G. In the bcChbC structure, G149S and K150E correspond to the loop that links TM6 and TM7 on the cytoplasmic side of the protein and S157F maps to the cytoplasmic end of TM7. M17 maps to the N terminal end of TM1, which is directly behind H250 on the cytoplasmic portion of TM6. H339Y and D343G map to

the second reentrant loop prior to HP2 (Fig. 7). Ruijter et al. found four mutations that facilitated transport in the absence of phosphorylation by the EIIB component [63]. Of these mutations, R203S and V206A map to the cytoplasmic end of TM6, K257N maps to the periplasmic half of TM8, and I296N maps to the first reentrant loop between HP1a and HP1b (Fig. 7).

Seven of these mutations correspond to the cytoplasmic end of the protein directly around the diacetylchitobiose molecule in the bcChbC structure. PtsG I296 (I332 in bcChbC) is highly conserved and located two residues prior to the conserved glutamate. In the bcChbC structure this isoleucine forms contacts with a series of hydrophobic residues on the loop between TM4 and TM5. G149S and K150E map to the TM4–TM5 loop directly across from the sugar. These mutations strongly suggest that some movement in this region is required for translocation of the sugar. Based on the bcChbC structure, the loop connecting TM4 and TM5 appears to be the most likely candidate for a cytoplasmic gate. A slight repositioning of the loop, possibly through the straightening of a kink in TM5 would allow egress of the sugar.

Two of the remaining mutations that influenced PtsG transport map to the second reentrant loop containing HP2 (H339Y and D343G). The last (K257N) maps to the periplasmic half of TM8. In our predicted model of the outward open state we would expect these regions to
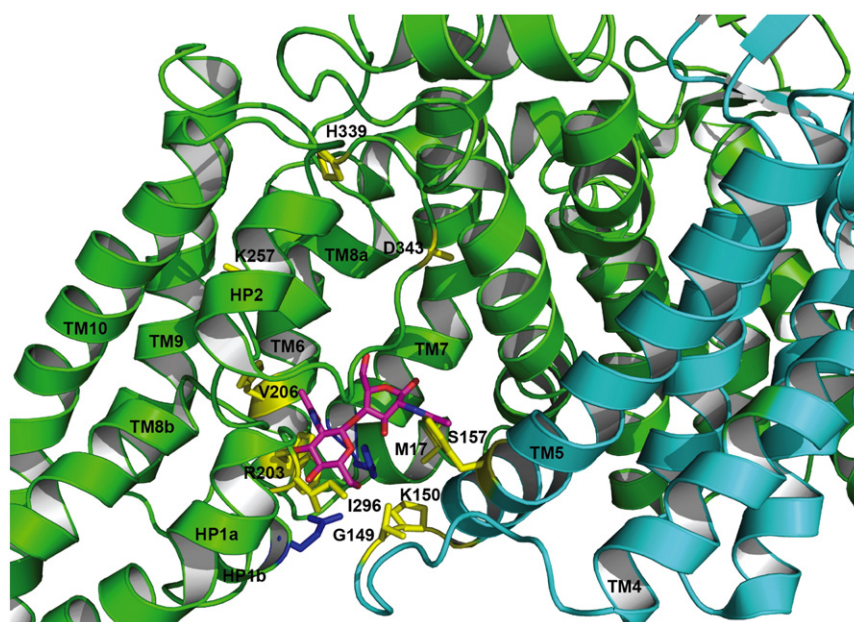


**Fig. 7.** Putative bcChbC gates controlling sugar entry and exit from the transporter. Residues that align in sequence with mutations in PtsG that affect transport are colored yellow and labeled according to the PtsG sequence. Protomer 1 is green, protomer 2 is cyan, N,N′-diacetylchitobiose is magenta, and E334 and H250 are shown in blue.

undergo large motions away from the oligomerization domain of the protein. In particular, H339 and D343 map to the interface between the binding and oligomerization domains, and mutations to those residues could therefore have an effect on the ability of the two domains to move relative to each other.

### 5.3. Transport in MtlA

Much of what is currently known about transport in EIIC proteins is based on studies of MtlA. Initial kinetic analysis of both PtsG and MtlA demonstrated biphasic behavior, suggesting the presence of multiple binding sites with differing affinities [49,64–66]. A more recent study concluded that MtlA has only one high affinity binding site per dimer ($K_D \approx 100$ nM) and that variations in the binding affinity constant were caused by contamination from an endogenous ligand [67]. Endogenous bound ligand has also been reported for PtsG [68]. The discovery that the mannitol binding site was positioned asymmetrically within the MtlA dimer led to the further hypothesis that the protomers acted in an alternating fashion, with passage of mannitol through one protomer causing it to switch from high affinity to low affinity and consequently driving the other protomer from a low affinity to a high affinity state capable of binding ligand [69]. This differs from what was observed in the bcChbC crystal structure in which the sugar molecule was bound to both protomers in a symmetric fashion. There is currently no evidence of cooperativity in the bcChbC dimer; however, given that the cytoplasmic gate appears to be supplied by the opposing protomer, it is possible that this could provide a mechanism for cooperativity, as sugar exiting the cavity of one protomer could be sensed by the other. Furthermore, residues in the N-terminal half of MtlA (the region corresponding from TM1 to TM4 in bcCHBC) were shown to be in close contact with mannitol, the sugar was shown to be located closer to the periplasm, and substantial differences were observed between solvent exposed residues in MtlA and their expected counterparts in the bcChbc structure [69,70]. Tryptophan phosphorescence spectroscopy indicated that F97 in MtlA (a predicted cytoplasmic loop residue that overlays TM3 in bcChbC) is part of a β-sheet fold [71]. Interestingly, this region was shown to undergo large conformational changes upon ligand binding with partial unfolding around F97, indicating that what appears to be essentially a dimerization domain in bcChbC may play a more extensive role in sugar translocation in MtlA [71]. This may be indicative of MtlA being in a different conformational state, or as discussed above, MtlA may be structurally distinct from bcChbC.

## 6. Conclusion

The bcChbC crystal structure has provided an initial framework for understanding over 20 years of functional work on properties of the glucose superfamily of EIIC transporters, including substrate selectivity, the phosphorylation reaction, and the mechanism of transport. However, the glucose superfamily is incredibly diverse and there is a high likelihood that different family members, in particular the mannitol and ß-glucoside families, may not share all the core structural features of bcChbC. Further determination of structures revealing variations in topology, different conformational states, and the nature of the EIIB and EIIC interaction are critical for understanding these proteins that form an essential component of bacterial carbohydrate regulation.

## Acknowledgements

## References

[1] J. Deutscher, C. Francke, P.W. Postma, How phosphotransferase system-related protein phosphorylation regulates carbohydrate metabolism in bacteria, Microbiol. Mol. Biol. Rev. 70 (2006) 939–1031.

[2] J.W. Lengeler, K. Jahreis, Bacterial PEP-dependent carbohydrate:phosphotransferase systems couple sensing and global control mechanisms, Contrib. Microbiol. 16 (2009) 65–87.

[3] P. Joyet, H. Bouraoui, F.M. Ake, M. Derkaoui, A.C. Zebre, T.N. Cao, M. Ventroux, S. Nessler, M.F. Noirot-Gros, J. Deutscher, E. Milohanic, Transcription regulators controlled by interaction with enzyme IIB components of the phosphoenolpyruvate: sugar phosphotransferase system, Biochim. Biophys. Acta 1834 (2013) 1415–1424.

[4] A.B. Chang, R. Lin, W. Keith Studley, C.V. Tran, M.H. Saier Jr., Phylogeny as a guide to structure and function of membrane transport proteins, Mol. Membr. Biol. 21 (2004) 171–181.

[5] M.H. Saier, R.N. Hvorup, R.D. Barabote, Evolution of the bacterial phosphotransferase system: from carriers and enzymes to group translocators, Biochem. Soc. Trans. 33 (2005) 220–224.

[6] T.X. Nguyen, M.R. Yen, R.D. Barabote, M.H. Saier Jr., Topological predictions for integral membrane permeases of the phosphoenolpyruvate:sugar phosphotransferase system, J. Mol. Microbiol. Biotechnol. 11 (2006) 345–360.

[7] H.R. Kaback, The role of the phosphoenolpyruvate–phosphotransferase system in the transport of sugars by isolated membrane preparations of *Escherichia coli*, J. Biol. Chem. 243 (1968) 3711–3724.

[8] G.S. Begley, D.E. Hansen, G.R. Jacobson, J.R. Knowles, Stereochemical course of the reactions catalyzed by the bacterial phosphoenolpyruvate:glucose phosphotransferase system, Biochemistry 21 (1982) 5552–5556.

[9] R.L. van Montfort, T. Pijning, K.H. Kalk, J. Reizer, M.H. Saier Jr., M.M. Thunnissen, G.T. Robillard, B.W. Dijkstra, The structure of an energy-coupling protein from bacteria. IIBcellobiose, reveals similarity to eukaryotic protein tyrosine phosphatases, Structure 5 (1997) 217–225.

[10] G.L. Orriss, B. Erni, T. Schirmer, Crystal structure of the IIB(Sor) domain of the sorbose permease from *Klebsiella pneumoniae* solved to 1.75 Å resolution, J. Mol. Biol. 327 (2003) 1111–1119.

[11] R.L. van Montfort, T. Pijning, K.H. Kalk, I. Hangyi, M.L. Kouwijzer, G.T. Robillard, B.W. Dijkstra, The structure of the *Escherichia coli* phosphotransferase IIAmannitol reveals a novel fold with two conformations of the active site, Structure 6 (1998) 377–388.

[12] S. Schauder, R.S. Nunn, R. Lanz, B. Erni, T. Schirmer, Crystal structure of the IIB subunit of a fructose permease (IIBLev) from *Bacillus subtilis*, J. Mol. Biol. 276 (1998) 591–602.

[13] R.S. Nunn, Z. Markovic-Housley, J.C. Genovesio-Taverne, K. Flukiger, P.J. Rizkallah, J. N. Jansonius, T. Schirmer, B. Erni, Structure of the IIA domain of the mannose transporter from *Escherichia coli* at 1.7 Angstroms resolution, J. Mol. Biol. 259 (1996) 502–511.

[14] P. Sliz, R. Engelmann, W. Hengstenberg, E.F. Pai, The structure of enzyme IIAlactose from *Lactococcus lactis* reveals a new fold and points to possible interactions of a multicomponent system, Structure 5 (1997) 775–788.

[15] D. Worthylake, N.D. Meadow, S. Roseman, D.I. Liao, O. Herzberg, S.J. Remington, Three-dimensional structure of the *Escherichia coli* phosphocarrier protein IIIglc, Proc. Natl. Acad. Sci. U. S. A. 88 (1991) 10382–10386.

[16] D.I. Liao, G. Kapadia, P. Reddy, M.H. Saier Jr., J. Reizer, O. Herzberg, Structure of the IIA domain of the glucose permease of *Bacillus subtilis* at 2.2-Å resolution, Biochemistry 30 (1991) 9583–9594.

[17] K. Schnetz, S.L. Sutrina, M.H. Saier Jr., B. Rak, Identification of catalytic residues in the beta-glucoside permease of *Escherichia coli* by site-specific mutagenesis and demonstration of interdomain cross-reactivity between the beta-glucoside and glucose systems, J. Biol. Chem. 265 (1990) 13464–13471.

[18] P.L. Grisafi, A. Scholle, J. Sugiyama, C. Briggs, G.R. Jacobson, J.W. Lengeler, Deletion mutants of the *Escherichia coli* K-12 mannitol permease: dissection of transport-phosphorylation, phospho-exchange, and mannitol-binding activities, J. Bacteriol. 171 (1989) 2719–2727.

[19] M. Meins, P. Jeno, D. Muller, W.J. Richter, J.P. Rosenbusch, B. Erni, Cysteine phosphorylation of the glucose transporter of *Escherichia coli*, J. Biol. Chem. 268 (1993) 11604–11609.

[20] A. Buhr, K. Flukiger, B. Erni, The glucose transporter of *Escherichia coli*. Overexpression, purification, and characterization of functional domains, J. Biol. Chem. 269 (1994) 23437–23443.

[21] Q. Chen, O. Amster-Choder, The different functions of BglF, the *E. coli* beta-glucoside permease and sensor of the bgl system, have different structural requirements, Biochemistry 37 (1998) 17040–17047.

[22] Q. Chen, O. Amster-Choder, BglF, the sensor of the bgl system and the beta-glucosides permease of *Escherichia coli*: evidence for dimerization and intersubunit phosphotransfer, Biochemistry 37 (1998) 8714–8723.

[23] J.S. Lolkema, G.T. Robillard, Subunit structure and activity of the mannitol-specific enzyme II of the *Escherichia coli* phosphoenolpyruvate-dependent phosphotransferase system solubilized in detergent, Biochemistry 29 (1990) 10120–10125.

[24] Y. Cao, X. Jin, E.J. Levin, H. Huang, Y. Zong, M. Quick, J. Weng, Y. Pan, J. Love, M. Punta, B. Rost, W.A. Hendrickson, J.A. Javitch, K.R. Rajashankar, M. Zhou, Crystal structure of a phosphorylation-coupled saccharide transporter, Nature 473 (2011) 50–54.

[25] U. Hummel, C. Nuoffer, B. Zanolari, B. Erni, A functional protein hybrid between the glucose transporter and the N-acetylglucosamine transporter of *Escherichia coli*, Protein Sci. 1 (1992) 356–362.

[26] J.S. Lolkema, D.S. Dijkstra, R.H. ten Hoeve-Duurkens, G.T. Robillard, The membrane-bound domain of the phosphotransferase enzyme IImtl of *Escherichia coli* constitutes a mannitol translocating unit, Biochemistry 29 (1990) 10659–10663.

[27] Y.S. Jung, M. Cai, G.M. Clore, Solution structure of the IIAChitobiose–IIBChitobiose complex of the N,N′-diacetylchitobiose branch of the *Escherichia coli* phosphotransferase system, J. Biol. Chem. 285 (2010) 4173–4184.

[28] M. Cai, D.C. Williams Jr., G. Wang, B.R. Lee, A. Peterkofsky, G.M. Clore, Solution structure of the phosphoryl transfer complex between the signal-transducing protein IIAGlucose and the cytoplasmic domain of the glucose transporter IICBGlucose of the *Escherichia coli* glucose phosphotransferase system, J. Biol. Chem. 278 (2003) 25191–25206.

[29] J.Y. Suh, M. Cai, D.C. Williams Jr., G.M. Clore, Solution structure of a post-transition state analog of the phosphotransfer reaction between the A and B cytoplasmic domains of the mannitol transporter IIMannitol of the *Escherichia coli* phosphotransferase system, J. Biol. Chem. 281 (2006) 8939–8949.

[30] S. Chen, M.L. Oldham, A.L. Davidson, J. Chen, Carbon catabolite repression of the maltose transporter revealed by X-ray crystallography, Nature 499 (2013) 364–368.

[31] J.M. Jeckelmann, D. Harder, S.A. Mari, M. Meury, Z. Ucurum, D.J. Muller, B. Erni, D. Fotiadis, Structure and function of the glucose PTS transporter from *Escherichia coli*, J. Struct. Biol. 176 (2011) 395–403.

[32] R.I. Koning, W. Keegstra, G.T. Oostergetel, G. Schuurman-Wolters, G.T. Robillard, A. Brisson, The 5 A projection structure of the transmembrane domain of the mannitol transporter enzyme II, J. Mol. Biol. 287 (1999) 845–851.

[33] N.O. Keyhani, S. Roseman, Wild-type *Escherichia coli* grows on the chitin disaccharide, N,N′-diacetylchitobiose, by expressing the cel operon, Proc. Natl. Acad. Sci. U. S. A. 94 (1997) 14367–14371.

[34] N.O. Keyhani, L.X. Wang, Y.C. Lee, S. Roseman, The chitin disaccharide, N,N′-diacetylchitobiose, is catabolized by *Escherichia coli* and is transported/phosphorylated by the phosphoenolpyruvate:glycose phosphotransferase system, J. Biol. Chem. 275 (2000) 33084–33090.

[35] Q.P. Weng, J. Elder, G.R. Jacobson, Site-specific mutagenesis of residues in the *Escherichia coli* mannitol permease that have been suggested to be important for its phosphorylation and chemoreception functions, J. Biol. Chem. 267 (1992) 19529–19535.

[36] Q.P. Weng, G.R. Jacobson, Role of a conserved histidine residue, His-195, in the activities of the *Escherichia coli* mannitol permease, Biochemistry 32 (1993) 11211–11216.

[37] R. Lanz, B. Erni, The glucose transporter of the *Escherichia coli* phosphotransferase system. Mutant analysis of the invariant arginines, histidines, and domain linker, J. Biol. Chem. 273 (1998) 12239–12243.

[38] C.A. Saraceni-Richards, G.R. Jacobson, A conserved glutamate residue, Glu-257, is important for substrate binding and transport by the *Escherichia coli* mannitol permease, J. Bacteriol. 179 (1997) 1135–1142.

[39] C.A. Saraceni-Richards, G.R. Jacobson, Subunit and amino acid interactions in the *Escherichia coli* mannitol permease: a functional complementation study of coexpressed mutant permease proteins, J. Bacteriol. 179 (1997) 5171–5177.

[40] A. Buhr, B. Erni, Membrane topology of the glucose transporter of *Escherichia coli*, J. Biol. Chem. 268 (1993) 11599–11603.

[41] S. Yagur-Kroll, O. Amster-Choder, Dynamic membrane topology of the *Escherichia coli* beta-glucoside transporter BglF, J. Biol. Chem. 280 (2005) 19306–19318.

[42] S. Yagur-Kroll, A. Ido, O. Amster-Choder, Spatial arrangement of the beta-glucoside transporter from *Escherichia coli*, J. Bacteriol. 191 (2009) 3086–3094.

[43] C.A. Lee, M.H. Saier Jr., Mannitol-specific enzyme II of the bacterial phosphotransferase system. III. The nucleotide sequence of the permease gene, J. Biol. Chem. 258 (1983) 10761–10767.

[44] J.E. Sugiyama, S. Mahmoodian, G.R. Jacobson, Membrane topology analysis of *Escherichia coli* mannitol permease by using a nested-deletion method to create mtlA–phoA fusions, Proc. Natl. Acad. Sci. U. S. A. 88 (1991) 9603–9607.

[45] E.B. Vervoort, J.B. Bultema, G.K. Schuurman-Wolters, E.R. Geertsma, J. Broos, B. Poolman, The first cytoplasmic loop of the mannitol permease from *Escherichia coli* is accessible for sulfhydryl reagents from the periplasmic side of the membrane, J. Mol. Biol. 346 (2005) 733–743.

[46] D.S. Dijkstra, J. Broos, J.S. Lolkema, H. Enequist, W. Minke, G.T. Robillard, A fluorescence study of single tryptophan-containing mutants of enzyme IImtl of the *Escherichia coli* phosphoenolpyruvate-dependent mannitol transport system, Biochemistry 35 (1996) 6628–6634.

[47] A. Krogh, B. Larsson, G. von Heijne, E.L. Sonnhammer, Predicting transmembrane protein topology with a hidden Markov model: application to complete genomes, J. Mol. Biol. 305 (2001) 567–580.

[48] B.A. van Montfort, G.K. Schuurman-Wolters, J. Wind, J. Broos, G.T. Robillard, B. Poolman, Mapping of the dimer interface of the *Escherichia coli* mannitol permease by cysteine cross-linking, J. Biol. Chem. 277 (2002) 14717–14723.

[49] L.F. Garcia-Alles, A. Zahn, B. Erni, Sugar recognition by the glucose and mannose permeases of *Escherichia coli* steady-state kinetics and inhibition studies, Biochemistry 41 (2002) 10077–10086.

[50] J.S. Lolkema, D.S. Dijkstra, R.H. ten Hoeve-Duurkens, G.T. Robillard, Interaction between the cytoplasmic and membrane-bound domains of enzyme IImtl of the *Escherichia coli* phosphoenolpyruvate-dependent phosphotransferase system, Biochemistry 30 (1991) 6721–6726.

[51] W. Meijberg, G.K. Schuurman-Wolters, G.T. Robillard, Thermodynamic evidence for conformational coupling between the B and C domains of the mannitol transporter of *Escherichia coli*, enzyme IImtl, J. Biol. Chem. 273 (1998) 7949–7956.

[52] B.A. van Montfort, G.K. Schuurman-Wolters, R.H. Duurkens, R. Mensen, B. Poolman, G.T. Robillard, Cysteine cross-linking defines part of the dimer and B/C domain interface of the *Escherichia coli* mannitol permease, J. Biol. Chem. 276 (2001) 12756–12763.

[53] E. Ab, G. Schuurman-Wolters, J. Reizer, M.H. Saier, K. Dijkstra, R.M. Scheek, G.T. Robillard, The NMR side-chain assignments and solution structure of enzyme IIBcellobiose of the phosphoenolpyruvate-dependent phosphotransferase system of *Escherichia coli*, Protein Sci. 6 (1997) 304–314.

[54] E. Ab, G.K. Schuurman-Wolters, D. Nijlant, K. Dijkstra, M.H. Saier, G.T. Robillard, R.M. Scheek, NMR structure of cysteinyl-phosphorylated enzyme IIB of the N,N′-diacetylchitobiose-specific phosphoenolpyruvate-dependent phosphotransferase system of *Escherichia coli*, J. Mol. Biol. 308 (2001) 993–1009.

[55] X.D. Su, N. Taddei, M. Stefani, G. Ramponi, P. Nordlund, The crystal structure of a low-molecular-weight phosphotyrosine protein phosphatase, Nature 370 (1994) 575–578.

[56] Y. Zhang, I-TASSER server for protein 3D structure prediction, BMC Bioinformatics 9 (2008) 40.

[57] Y. Yamada, Y.Y. Chang, G.A. Daniels, L.F. Wu, J.M. Tomich, M. Yamada, M.H. Saier Jr., Insertion of the mannitol permease into the membrane of *Escherichia coli*. Possible involvement of an N-terminal amphiphilic sequence, J. Biol. Chem. 266 (1991) 17863–17871.

[58] L. Wu, Z.Y. Zhang, Probing the function of Asp128 in the lower molecular weight protein-tyrosine phosphatase-catalyzed reaction. A pre-steady-state and steady-state kinetic investigation, Biochemistry 35 (1996) 5426–5434.

[59] Z.Y. Zhang, Y. Wang, L. Wu, E.B. Fauman, J.A. Stuckey, H.L. Schubert, M.A. Saper, J.E. Dixon, The Cys(X)5Arg catalytic motif in phosphoester hydrolysis, Biochemistry 33 (1994) 15266–15270.

[60] A.P. Jackson, A. Maxwell, Identifying the catalytic residue of the ATPase reaction of DNA gyrase, Proc. Natl. Acad. Sci. U. S. A. 90 (1993) 11232–11236.

[61] N. Reyes, C. Ginter, O. Boudker, Transport mechanism of a bacterial homologue of glutamate transporters, Nature 462 (2009) 880–885.

[62] A. Buhr, G.A. Daniels, B. Erni, The glucose transporter of *Escherichia coli*. Mutants with impaired translocation activity that retain phosphorylation activity, J. Biol. Chem. 267 (1992) 3847–3851.

[63] G.J. Ruijter, G. van Meurs, M.A. Verwey, P.W. Postma, K. van Dam, Analysis of mutations that uncouple transport from phosphorylation in enzyme IIGlc of the *Escherichia coli* phosphoenolpyruvate-dependent phosphotransferase system, J. Bacteriol. 174 (1992) 2843–2850.

[64] L.F. Garcia-Alles, V. Navdaeva, S. Haenni, B. Erni, The glucose-specific carrier of the *Escherichia coli* phosphotransferase system, Eur. J. Biochem. 269 (2002) 4969–4980.

[65] J.S. Lolkema, R.H. ten Hoeve-Duurkens, G.T. Robillard, Steady state kinetics of mannitol phosphorylation catalyzed by enzyme IImtl of the *Escherichia coli* phosphoenolpyruvate-dependent phosphotransferase system, J. Biol. Chem. 268 (1993) 17844–17849.

[66] M.G. Elferink, A.J. Driessen, G.T. Robillard, Functional reconstitution of the purified phosphoenolpyruvate-dependent mannitol-specific transport system of *Escherichia coli* in phospholipid vesicles: coupling between transport and phosphorylation, J. Bacteriol. 172 (1990) 7119–7125.

[67] G. Veldhuis, J. Broos, B. Poolman, R.M. Scheek, Stoichiometry and substrate affinity of the mannitol transporter, EnzymeIImtl, from *Escherichia coli*, Biophys. J. 89 (2005) 201–210.

[68] N.D. Meadow, R.S. Savtchenko, A. Nezami, S. Roseman, Transient state kinetics of enzyme IICBGlc, a glucose transporter of the phosphoenolpyruvate phosphotransferase system of *Escherichia coli*: equilibrium and second order rate constants for the glucose binding and phosphotransfer reactions, J. Biol. Chem. 280 (2005) 41872–41880.

[69] M. Opacic, E.P. Vos, B.H. Hesp, J. Broos, Localization of the substrate-binding site in the homodimeric mannitol transporter, EIImtl, of *Escherichia coli*, J. Biol. Chem. 285 (2010) 25324–25331.

[70] M. Opacic, B.H. Hesp, F. Fusetti, B.W. Dijkstra, J. Broos, Structural investigation of the transmembrane C domain of the mannitol permease from *Escherichia coli* using 5-FTrp fluorescence spectroscopy, Biochim. Biophys. Acta 1818 (2012) 861–868.

[71] G. Veldhuis, E. Gabellieri, E.P. Vos, B. Poolman, G.B. Strambini, J. Broos, Substrate-induced conformational changes in the membrane-embedded IIC(mtl)-domain of the mannitol permease from *Escherichia coli*, EnzymeII(mtl), probed by tryptophan phosphorescence spectroscopy, J. Biol. Chem. 280 (2005) 35148–35156.